FEBS Letters 577 (2004) 170–174 FEBS 28926

Structure of the mitochondrial β-ketoacyl-[acyl carrier protein] synthase from *Arabidopsis* and its role in fatty acid synthesis ☆

Johan G. Olsen[a], Anne V. Rasmussen[b], Penny von Wettstein-Knowles[b], Anette Henriksen[a,*]

[a] *Carlsberg Laboratory, Gamle Carlsberg Vej 10, DK-2500 Valby, Denmark*
[b] *Institute of Molecular Biology, University of Copenhagen, Øster Farimagsgade 2A, DK-1353 Copenhagen K, Denmark*

Received 20 August 2004; revised 24 September 2004; accepted 1 October 2004

Available online 14 October 2004

Edited by Gerrit van Meer

Abstract Mitochondrial fatty acid synthesis is catalyzed by a dissociated fatty acid synthase similar to those of plant plastids and bacteria. The crystal structure of a mitochondrial β-ketoacyl-[acyl carrier protein] synthase (mtKAS), namely that from *Arabidopsis thaliana*, has been determined for the first time. This enzyme accomplishes the vital condensation steps in constructing fatty acid carbon skeletons. The product profile of mtKAS is unusual in that C_8 and $C_{14–16}$ fatty acyl chains predominate. An enzyme architecture that likely is the basis for the observed bimodal profile of mtKAS products can be derived from the shape of the acyl binding pocket.

Keywords: Mitochondrial β-ketoacyl-ACP synthase; Lipoic acid; Cerulenin sensitivity

1. Introduction

Fatty acid synthase (FAS) complexes consist of the small acyl carrier protein (ACP) cofactor and a set of enzymatic activities either gathered on very large multifunctional polypeptides (type I) or organized from discrete enzymes (type II). In a reiterative manner, short carbon units activated by ACP or coenzyme A are joined together by FAS and then prepared for the next round of elongation. For many years, the type I and II FAS systems were believed to be mutually exclusive, with type I occurring in the cytoplasm of animals and fungi [1], and with a few exceptions, type II in bacteria [2] and plastids [3]. Seeking an explanation for the presence of ACP in the mitochondria of *Neurospora crassa* [4], however, led to the identification of nuclear genes potentially encoding other components of type II FAS systems for the mitochondria of fungi, plants and animals [5–10]. Some of the products of these genes have been shown to carry mitochondrial targeting signals and have the requisite activities to function in fatty acid synthesis. Combining all possible observations leads to the inference that a mitochondrial FAS II system exists in all eukaryotes.

FAS is an interesting target for both cytostatica and antibiotics. Fatty acid synthesis is substantially elevated in tumor cells [11] and FAS inhibitors, such as the natural antibiotic cerulenin, impede tumor growth and induce apoptosis [12]. The differential sensitivity of FAS complexes to antibiotics makes FAS a favorable target for the development of antibiotics [13]. Cerulenin inhibits the condensing enzyme, β-ketoacyl-ACP synthase (KAS) component of FAS, performing the three step Claisen condensation reaction. Specifically, cerulen-in binds covalently to the active site cysteine, occupying the acyl binding pocket [14,15] and thereby prohibiting binding of the acyl substrate.

Among the best characterized of the mitochondrial type II FAS components is the KAS enzyme from *Arabidopsis thaliana*, mtKAS [10]. This enzyme, as KAS I of *Escherichia coli*, is a promiscuous condensing enzyme accepting $C_{4–14}$ acyl substrates. The enzymes differ in that mtKAS also extends saturated C_2 and C_{16} acyl chains [10], while KAS I elongates unsaturated $C_{10:1–14:1}$ acyl chains [16]. *E. coli* KAS II is similar to KAS I except for selecting $C_{16:1}$ rather than $C_{10:1}$-$C_{14:1}$ acyl chains [16]. A second attribute distinguishing mtKAS from other KAS enzymes is the unusual product profile having two maxima, one with C_8 and one with C_{14}–C_{18} acyl chains [10,17]. While the former are precursors for lipoic acid [17], the function of the longer acyl chains remains to be demonstrated. Their participation in phospholipid remodeling has been proposed [18].

Crystal structures determined for the *E. coli* KAS I [19] and for KAS II from *E. coli* [20], *Streptococcus pneumoniae* [21] and *Synechocystis* sp. [22] have not clarified the structural basis for substrate preferences of these enzymes. The current work presents the first successful purification of a KAS enzyme from a eukaryotic type II FAS, namely the *A. thaliana* mtKAS, leading to the determination of its molecular structure. Superimposing the cerulenin complexed structures of *E. coli* KAS I and II on the acyl binding pocket of mtKAS reveals not only the likely basis for the bimodal product distribution, but also a factor contributing to the extreme sensitivity of mtKAS to the inhibitor cerulenin.

2. Materials and methods

2.1. Cloning, expression, and purification of recombinant protein

DNA encoding a truncated version of *A. thaliana* cDNA AB073746 encoding mtKAS was recloned from pKK233-2 [10] into pQE30 (Qiagen). The mtKASΔ20 sequence, lacking the first 20 codons of the

☆ The coordinates and structure factors have been deposited in the Protein Data Bank at EBI (http://www.ebi.ac.uk/msd) as entry 1W0I.

* Corresponding author. Fax: +45-33274708.
E-mail address: anette@crc.dk (A. Henriksen).

Abbreviations: ACP, acyl carrier protein; cerulenin, (2*R*,3*S*)-2,3-epoxy-4-oxo-7,10-dodecandienoylamide; FAS, fatty acid synthase; KAS, β-ketoacyl acyl carrier protein synthase; MES, 2-[*N*-morpholino]propanesulfonic acid; mtKAS, mitochondrial KAS; Tris–HCl, tris[hydroxymethyl]aminomethane hydrochloride

0014-5793/$22.00
doi:10.1016/j.febslet.2004.10.007

Table 1
Data collection and refinement statistics

	Native 1	Native 2	Native 3	Native 4	Merged data
Data collection					
Beam line	DESY/X13	DESY/X13	DESY/X13	ESRF/BM14	
Wavelength (Å)	0.802	0.802	0.802	0.984	
Cell dimensions	$a = 71.8$ Å $b = 92.8$ Å $c = 73.4$ Å $\beta = 106.4°$	$a = 71.8$ Å $b = 92.8$ Å $c = 73.5$ Å $\beta = 106.4°$	$a = 71.8$ Å $b = 92.7$ Å $c = 73.5$ Å $\beta = 106.4°$	$a = 72.2$ Å $b = 93.2$ Å $c = 74.0$ Å $\beta = 106.4°$	
Resolution range (last shell) (Å)	20.1–2.4 (2.5–2.4)	20.7–2.5 (2.6–2.5)	20.9–3.0 (3.2–3.0)	36.5–2.1 (2.2–2.1)	23.6–2.1 (2.2–2.1)
Number of unique reflection	13 076	7468	2065	31 170	42 636
R_{merge} (last shell)[a]	0.133 (0.360)	0.130 (0.351)	0.199 (0.466)	0.098 (0.259)	0.145 (0.262)
Multiplicity	1.7	1.7	1.5	1.9	3.5
Completeness (%)	61.0	49.0	30.1	89.0	95.4
Average I/σ	5.3	5.2	3.6	3.4	4.4
Refinement statistics					
Number of reflections				52211	
Resolution range (last shell) (Å)				23.7–2.10 (2.19–2.10)	
Number of non-hydrogen protein atoms				6430	
Number of atoms in ions				17	
Number of water molecules				565	
R-factor[b]				17.8	
R_{free}[b]				22.1	
Cross-validated estimated coordinate error using σ (Å)[c]				0.2	
rmsd					
Bond length (Å)[c]				0.006	
Bond angle (°)[c]				1.2	
Dihedral angle (°)[c]				22.8	
Improper torsion (°)[c]				0.8	
Average B					
Protein (Å^2)				12.4	
Water (Å^2)				23.3	
Ions (Å^2)				31.7	
rmsd between ncs-related subunits (Å)				0.3	

[a] $R_{merge} = \sum_{hkl}\sum_i |I_i(hkl) - \langle I_i(hkl)\rangle| / \sum_{hkl}\sum_i I_i(hkl)$.
[b] R-factor $= \sum_{hkl} ||F_{obs}| - |F_{calc}|| / \sum_{hkl} |F_{obs}|$, with R_{free} calculated using 5% of the reflections held aside during the refinement process.
[c] Calculated in CNS [28].

mtKAS cDNA, was amplified by PCR with the primers 5′ *Bam*HI, 5′-GGTGGTGGT**GGATCC**ATCTCTACTTCTTCTTC-3′ and 3′ *Pst*I 5′-GAAGCTTGG**CTGCAG**TTAGATAGATAG-3′, and subcloned into pQE30 (Qiagen). The resulting pQEmtKAS vector, encoding an MRGSHHHHHHG N-terminal sequence preceding that of mtKASΔ20, was transformed using standard techniques into C41(DE3) cells previously transformed with pREP4 (Qiagen).

Expression was carried out as previously described [23], excepting that induction was optimized by overnight incubation at 20 °C to avoid inclusion of body formation. After cell disruption by lysozyme treatment, followed by endonuclease treatment and centrifugation, the supernatant was subject to Ni^{2+} affinity chromatography on a 5 mL HiTrap chelating HP column (all columns were from Amersham Biosciences). After buffer exchange [to 30 mM Tris–HCl (tris[hydroxymethyl]aminomethane hydrochloride), 2 mM EDTA, and 1 mM DTT, pH 8.0] on a HiPrep 26/10 desalting column, the protein was further purified by ion exchange chromatography on a MonoQ HR10/10 column. The purified enzyme was buffer exchanged on a HiPrep 26/10 desalting column into 30 mM Tris–HCl, 2 mM EDTA, and 1 mM DTT (pH 8.0) and concentrated to 16.3 mg/mL based on a theoretical $A_{280}^{1\,mg/mL} = 0.467$.. This procedure yielded a total of 2 mg mtKAS from 1 L cell culture.

2.2. Crystallization and data collection

Hanging drop experiments using equal volumes of mother liquor and protein solution equilibrated against 1.6 M $(NH_4)_2SO_4$ and 0.1 M MES (2-[*N*-morpholino]propanesulfonic acid)-buffer at pH 6.0 lead to elongated plate shaped crystals with average dimensions of 0.4

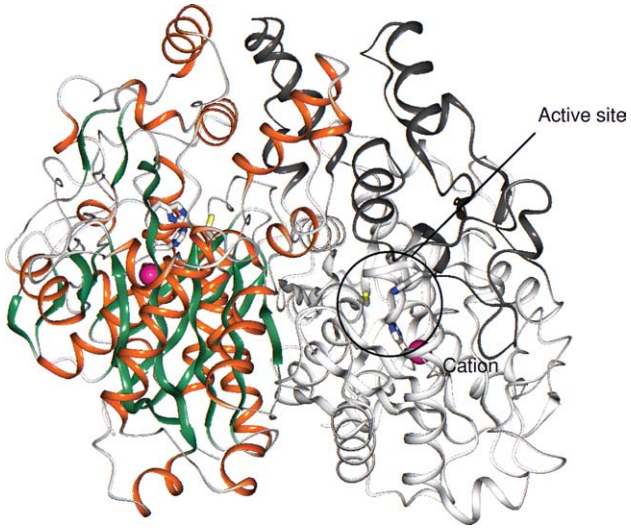

Fig. 1. Ribbon representation of *A. thaliana* mtKAS. Active site Cys209, His350 and His389 are included. One subunit is colored according to secondary structural elements, while in the other subunit the core αβαβα structure is white and the cap region is dark gray. The purple spheres represent cations inferred to be K^+.

mm × 0.05 mm × 0.01 mm. The crystals were cooled in $N_{2(l)}$ after transfer to a cryo-protectant consisting of 1.6 M $(NH_4)_2SO_4$, 0.1 M MES-buffer and 25% (v/v) glycerol at pH 6.0. Exposure of the crystals to X-ray radiation resulted in severe crystal damage and a full data set from the exposure of a single crystal was unobtainable. Consequently, the data from four crystals were scaled and merged. Data from one crystal were collected at ESRF beam line BM14 and from three other crystals at DESY beam line X11 (Table 1). The space group of the crystals is $P2_1$ with $a = 71.8$ Å, $b = 92.8$ Å, $c = 73.4$ Å, and $\beta = 106.4°$, making room for one mtKAS dimer in the asymmetric unit.

2.3. Phasing, model building and refinement

Escherichia coli KAS I, pdb code 1EK4 [24] was used as search model for the initial phase estimation by molecular replacement [25]. Phases were improved by automated model building in ARP/wARP [26], and complete protein chains constructed after model building in O [27] and model refinement in CNS [28]. After inclusion of water molecules, five of them appeared more likely to be ions because of very low *B*-factors, the shape of the electron density and the number and organization of coordinating atoms. Three sulfate ions, two in the A subunit and one in *B*, were included at the molecular surface, all with salt bridges to arginine residues. A K^+ ion in each subunit was included in the intramolecular cation site previously observed in *Streptococcus pneumoniae* KAS II [21]. The identification of the cation in mtKAS is based on model refinement trials including NH_4^+ ($\langle B_{factor}\rangle = 1.7$ Å^2), Na^+ ($\langle B_{factor}\rangle = 14.6$ Å^2), K^+ ($\langle B_{factor}\rangle = 22.7$ Å^2), Ca^{2+} ($\langle B_{factor}\rangle = 23.0$ Å^2) or Mg^{2+} ($\langle B_{factor}\rangle = 13.3$ Å^2), assuming 100% occupancy of the site. The average cation ligand distance of 2.8 Å suggests an NH_4^+ or K^+ ion [29]. The non-realistic low *B*-factor of the NH_4^+ model (reset to 1.7 Å^2 after having dropped below the *B*-factor limit in the refinement procedure), however, argues for the more electron dense K^+, possibly partly occupied. Alternating occupancy and B_{factor} refinement of the K^+ model gave converged occupancies of 0.5/0.6 with corresponding *B*-factors of 7.1 Å^2/9.3 Å^2. The side chain of Thr 354 was refined in two alternate conformations.

3. Results and discussion

3.1. Architecture of mtKAS

Two subunits of mtKAS are associated into a dimer in the asymmetric unit, with each subunit contributing to the dimer interface with an area of 3466 Å^2 [30]. This is 350–1200 Å^2 larger than the interfaces formed by other KAS I, II and III dimers. As in KAS I and KAS II structures, each subunit is organized in two entities, a large αβαβα sandwich carrying the active site residues and an α-helical cap above the active site (Fig. 1). The structure of mtKAS has two major structural extensions compared to KAS I and KAS II enzymes. These are an extra α-helical segment in the cap region contributing to the dimer interface (mtKAS residues 67–83) and a solvent exposed loop in the αβαβα domain (mtKAS residues 98–105) (Fig. 2). In addition, a minor extension is found in the 374–375 region. The dimer formation observed in all KAS enzymes plays a role for the definition of the fatty acyl binding pocket. With respect to overall size, position and hydrophobic nature, the mtKAS pocket resembles the KAS I and II pockets. At a more detailed level, several observations imply that mtKAS is closely related to KAS II. For example, the active site water structure of mtKAS resembles that observed in the KAS II enzymes from *T. thermophilus* (pdb code: 1j3n) and *Synechocystis* sp. [20], in particular no short hydrogen bonds are observed from active site residue His350 N_{D1}.

3.2. Substrate binding implications

Only hydrophobic residues line the mtKAS acyl pocket (Fig. 3A). Analogous residues in all other deduced mtKAS sequences [NCBI Accession Codes: CAA21898, P39525, AAB81078, BAB30490, BAA91286, CG12170-PA, XM_312104, AK116556, CE30752, F10G8.9(Z80216) and CBP01094] are also hydrophobic. By comparison, the bottom of this pocket in *E. coli* includes Glu200 and Gln113 in KAS I and Thr137 in KAS II (Figs. 3B and C, respectively).

Cerulenin inhibits KAS by binding covalently to the active site cysteine. The resulting complexes, for example those with *E. coli* KAS I and II [14,15], are products of a nucleophilic addition to the cerulenin epoxide, and not of a nucleophilic substitution characterizing the formation of KAS:fatty acyl complexes. Furthermore, the leaving group of the natural substrate ACP participates in the reaction [31]. The time course of the two reactions cannot be expected to be the same. The cerulenin complexes reveal that KAS II residues Ile108, Val134 and Ile138 (Gly107, Val134 and Met138 in KAS I) constrict the acyl binding pocket in two positions, and that the binding of cerulenin induces a reorientation of Ile108 needed to accommodate cerulenin atoms beyond the fatty acyl C_7 position, as illustrated in Fig. 3C. This rotation of Ile108 in *E. coli* KAS II was invoked to explain the far greater sensitivity to cerulenin of KAS I than KAS II [32].

Although orientation of the cerulenin C_ω-end varies, superimposition of the KAS I:cerulenin and KAS II:cerulenin complexes with mtKAS discloses a KAS II-like constriction of the acyl pocket in this enzyme just beyond the fatty acyl C_7

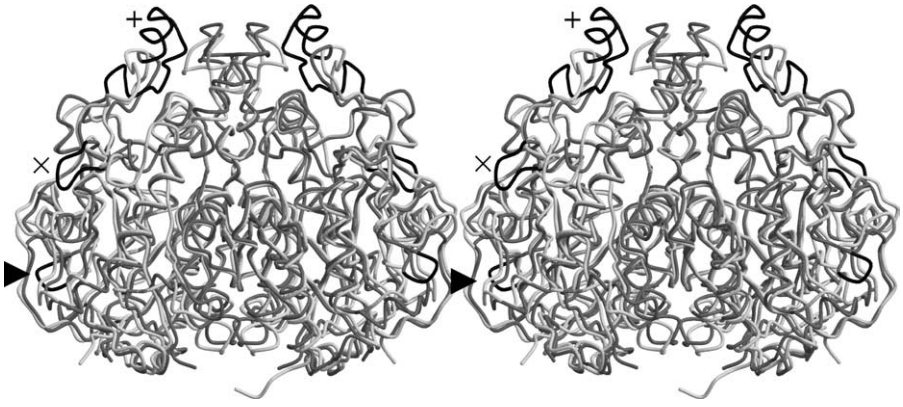

Fig. 2. Superposition of mtKAS (dark gray) and the high resolution structure of KAS II from *S. pneumoniae* (light gray) [21]. The parts of the mtKAS structure with the largest deviations from KAS II structures are colored black: +, residues 67–83; ×, residues 98–105; ▶, residues 374–375.

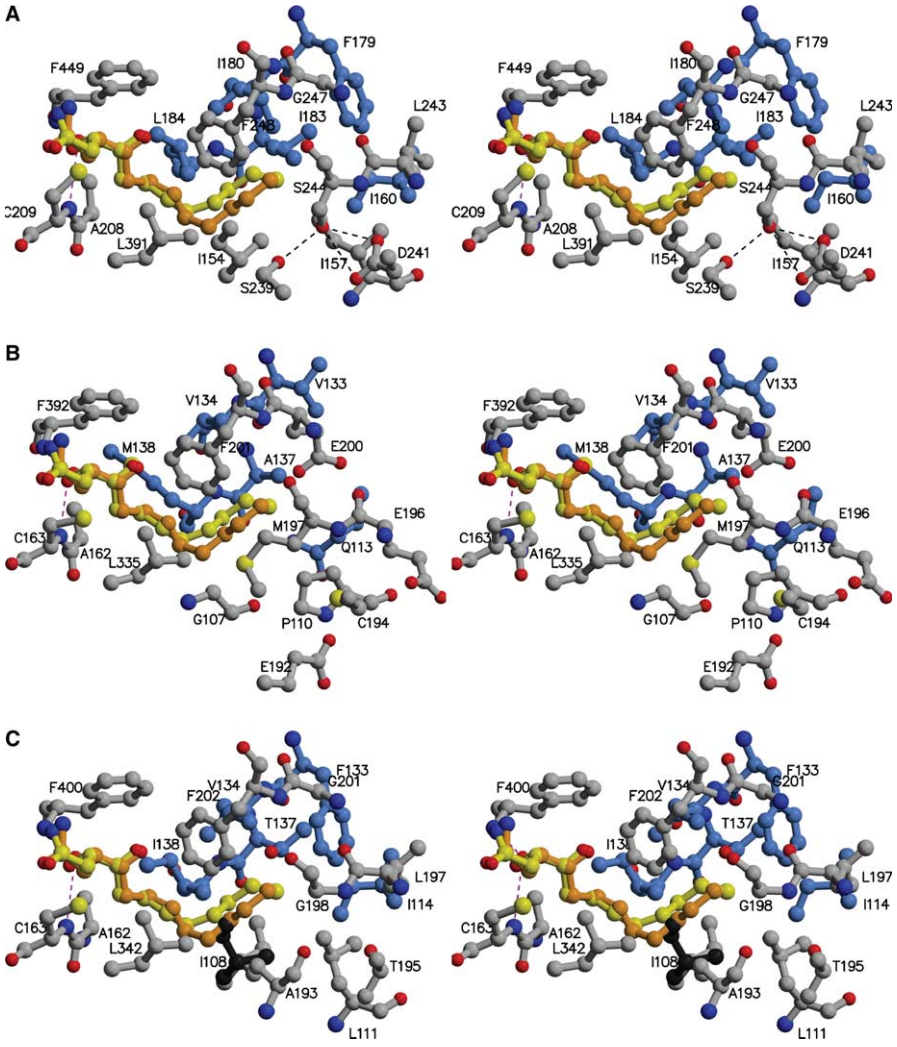

Fig. 3. KAS acyl binding pockets. The cerulenin chains from superimposed *E. coli* KAS I (yellow) and KAS II (orange) complexes have been included with potential hydrogen bonds (dotted lines) to the oxyanion hole (magenta). (A) *A. thaliana* mtKAS acyl binding pocket. (B) *E. coli* KAS I acyl binding pocket and (C) *E. coli* KAS II acyl binding pocket. The black side chain illustrates the orientation of Ile108 in the native KAS II structure. Light blue residues are from the B subunits, gray residues are from the A subunits. The sequence identity of mtKAS with *E. coli* KAS I and KAS II is 38% and 50%, respectively.

position (Fig. 3A). The mtKAS residues involved are Ile154, Ile180 and Leu184, and we expect cerulenin binding to mtKAS to involve a rotation of Ile154 analogous to that observed in KAS II (Fig. 3C). Since mtKAS is at least as sensitive to cerulenin as *E. coli* KAS I [10], the deduced rotation of Ile154 does not impede cerulenin binding in this enzyme. Although slightly less spacious, the completely hydrophobic acyl binding pocket defined by Ile154, Ile157, Ile180, Ile183, and Leu184 (Ile108, Leu111, Val134, Thr137 and Ile138 in KAS II) likely provides an almost perfect fit to the ligand with respect to shape and polarity, and hence favors inhibitor binding. We note that cerulenin C_ω is positioned as far as possible from Thr137 O_G (Ala137 in KAS I and Ile183 in mtKAS) in the KAS II:cerulenin C_ω complex, while in the KAS I:cerulenin complex it is oriented towards the structurally equivalent residue.

Also the bimodal product profile characterizing mtKAS, but not *E. coli* KAS II, indicates that reorientation of Ile154 to another tautomer has energetically different consequences in the two enzymes. Likely, no substantial energy barrier exists for reorientation of the constricting Ile residue in KAS II, while reorientation in the more narrow mtKAS pocket is energetically unfavorable. After Ile154 reorientation, the longer fatty acyl substrates gain access to the wider and solvent filled interior of the mtKAS pocket (Fig. 3A).

4. Conclusion

The very hydrophobic acyl binding pocket observed in this first structure of a mitochondrial KAS fits well with the observed sensitivity of the enzyme to the inhibitor cerulenin. The orientation of Ile154 in the constricted binding pocket suggests that this residue plays a major role for the bimodal product profile of the enzyme and its involvement in the formation of C_8-ACP for lipoic acid production.

Acknowledgements: This work was supported by Novo Nordisk Foundation and the Danish National Research Council. Financial support from DANSYNC and the EU, ARI program made data

collection possible. Beam line scientists Hassan Belrhali (beam line BM14, ESRF) and Alexander Popov (Beam line X11, DESY) are acknowledged for technical assistance during data collection and Drs. R. Yasuno and G. Besra are thanked for the pKK233Δ20mtKAS clone and the C41(DE3) cells, respectively.

References

[1] Smith, S. (1994) FASEB J. 8, 1248–1259.
[2] Rock, C.O. and Cronan, J.E. (1996) Biochim. Biophys. Acta 1302, 1–16.
[3] Harwood, J.L. (1988) Ann. Rev. Plant Physiol. Plant Mol. Biol. 39, 101–138.
[4] Chuman, L. and Brody, S. (1989) Eur. J. Biochem. 184, 643–649.
[5] Shintani, D.K. and Ohlrogge, J.B. (1994) Plant Physiol. 104, 1221–1229.
[6] Torkko, J.M., Koivuranta, K.T., Miinalainen, I.J., Yagi, A.I., Schmitz, W., Kastaniotis, A.J., Airenne, T.T., Gurvitz, A. and Hiltunen, K.J. (2001) Mol. Cell Biol. 21, 6243–6253.
[7] Miinalainen, I.J., Chen, Z.-J., Torkko, J.M., Pirila, P.L., Sormunen, R.T., Bergmann, U., Qin, Y.-M. and Hiltunen, J.K. (2003) J. Biol. Chem. 278, 20154–20161.
[8] Torkko, J.M., Koivuranta, K.T., Kastaniotis, A.J., Airenne, T.T., Glumoff, T., Ilves, M., Hartig, A., Gurvitz, A. and Hiltunen, J.K. (2003) J. Biol. Chem. 278, 41213–41220.
[9] Zhang, L., Joshi, A.K. and Smith, S. (2003) J. Biol. Chem. 278, 40067–40074.
[10] Yasuno, R., von Wettstein-Knowles, P. and Wada, H. (2004) J. Biol. Chem. 279, 8242–8251.
[11] Pflug, B.R., Pecher, S.M., Brink, A.W., Nelson, J.B. and Foster, B.A. (2003) Prostate 57, 245–254.
[12] Li, J.N., Gorospe, M., Chrest, F.J., Kumaravel, T.S., Evans, M.K., Han, W.F. and Pizer, E.S. (2001) Cancer Res. 61, 1493–1499.
[13] Phillips, O.A. and Matowe, W.C. (2002) Curr. Opin. Investig. Drugs 3, 1701–1711.
[14] Moche, A., Schneider, G., Edwards, P., Dehesh, K. and Lindqvist, Y. (1999) J. Biol. Chem. 274, 6031–6034.
[15] Price, A.C., Choi, K.-H., Heath, R.J., Li, Z., White, S.W. and Rock, C.O. (2001) J. Biol. Chem. 276, 6551–6559.
[16] Garwin, J.L., Klages, A.L. and Cronan, J.E. (1980) J. Biol. Chem. 255, 11949–11956.
[17] Gueguen, V., Macherel, D., Jaquinod, M., Douce, R. and Bourguignon, J. (2000) J. Biol. Chem. 275, 5016–5025.
[18] Schneider, R., Brors, B., Burger, F., Camrath, S. and Weiss, H. (1997) Curr. Genet. 32, 384–388.
[19] Olsen, J.G., Kadziola, A., von Wettstein-Knowles, P., Siggaard-Andersen, M. and Larsen, S. (2001) Structure 9, 233–243.
[20] Huang, W., Jia, J., Edwards, P., Dehesh, K., Schneider, G. and Lindqvist, Y. (1998) EMBO J. 17, 1183–1191.
[21] Price, A.C., Rock, C.O. and White, S.W. (2003) J. Bacteriol. 185, 4136–4143.
[22] Moche, M., Dehesh, K., Edwards, P. and Lindqvist, Y. (2001) J. Mol. Biol. 305, 491–503.
[23] McGuire, K.A., Siggaard-Andersen, M., Bangera, M.G., Olsen, J.G. and von Wettstein-Knowles, P. (2001) Biochemistry 40, 9836–9845.
[24] Olsen, J.G., Kadziola, A., von Wettstein-Knowles, P., Siggaard-Andersen, M., Lindquist, Y. and Larsen, S. (1999) FEBS Lett. 460, 46–52.
[25] Navaza, J. and Saludjian, P. (1997) Meth. Enzymol. 276, 581–594.
[26] Morris, R.J., Perrakis, A. and Lamzin, V.S. (2003) Meth. Enzymol. 374, 229–244.
[27] Jones, A., Zou, J.Y., Cowan, S.W. and Kjeldgaard, M. (1991) Acta Crystallogr. A 47, 110–119.
[28] Brünger, A.T., Adams, P.D., Clore, G.M., DeLano, W.L., Gros, P., Grosse-Kunstleve, R.W., Jiang, J.-S., Kuszewski, J., Nilges, M., Pannu, N.S., Read, R.J., Rice, L.M., Simonson, T. and Warren, G.L. (1998) Acta Crystallogr. D 54, 905–921.
[29] Harding, M.M. (2002) Acta Crystallogr. D 58, 872–874.
[30] Hubbard, S.J. and Thornton, J.M. (1999) NACCESS. Department of Biochemistry and Molecular Biology, University College, London.
[31] D'Agnolo, G., Rosenfeld, I.S. and Vagelos, P.R. (1975) J. Biol. Chem. 250, 5283–5288.
[32] Val, D., Banu, G., Seshadri, K., Lindqvist, Y. and Dehesh, K. (2000) Structure 8, 565–566.